Atmos. Chem. Phys. Discuss., 9, 22143–22175, 2009
www.atmos-chem-phys-discuss.net/9/22143/2009/

Atmospheric Chemistry and Physics Discussions

This discussion paper is/has been under review for the journal *Atmospheric Chemistry and Physics (ACP)*. Please refer to the corresponding final paper in *ACP* if available.

Toward a real-time measurement of atmospheric mercury concentrations using cavity ring-down spectroscopy

X. Faïn, H. Moosmüller, and D. Obrist

Division of Atmospheric Sciences, Desert Research Institute, 2215 Raggio Parkway, Reno, NV 89512, USA

Received: 2 October 2009 – Accepted: 5 October 2009 – Published: 21 October 2009

Correspondence to: X. Faïn (xavier.fain@dri.edu)

Published by Copernicus Publications on behalf of the European Geosciences Union.

Abstract

A new sensor based on cavity ring-down spectroscopy (CRDS) has been developed for the measurement of gaseous elemental mercury (Hg^0) mass concentration with sub-ng m^{-3} detection limit and high temporal resolution. Cavity ring-down spectroscopy is a direct absorption technique that utilizes path lengths of up to multiple kilometers in a compact absorption cell and has a significantly higher sensitivity than conventional absorption spectroscopy. Our prototype uses a frequency-doubled, tuneable dye laser emitting pulses at ~253.65 nm with a pulse repetition frequency of 50 Hz. The dye laser incorporates a unique piezo element attached to its tuning grating allowing it to tune the laser on and off the Hg^0 absorption line on a pulse to pulse basis to facilitate differential absorption measurements. Hg^0 absorption measurements with this CRDS laboratory prototype are highly linearly related to Hg^0 concentrations determined by a Tekran 2537B analyzer over a Hg^0 concentration range of four orders of magnitude, from 0.2 ng m^{-3} to 573 ng m^{-3} implying excellent linearity of both instruments. The current CRDS instrument has a sensitivity of 0.10 ng m^{-3} at 10 s time resolution. This tool opens new prospects for the study of Hg^0 because of its high temporal resolution and reduced limited sample volume requirements (<0.5 l of sample air). Future applications may include ambient Hg^0 flux measurements with eddy covariance techniques, which require measurements of Hg^0 concentrations with sub-ng m^{-3} sensitivity and sub-second time resolution.

1 Introduction

Mercury (Hg) is a toxic pollutant globally dispersed in the environment. Natural and anthropogenic sources emit mercury to the atmosphere, either as gaseous elemental mercury (GEM or Hg^0) or as divalent mercury species. Hg^0, which represents as much as 95% of the atmospheric mercury burden, has an atmospheric lifetime in the range of 5–24 months and can be transported across long distances to remote lo-

ACPD

9, 22143–22175, 2009

cations (Schroeder and Munthe, 1998). Measurements of atmospheric background levels of Hg^0 (~1.7 ng m^{-3}, Valente et al., 2007) currently require pre-concentration of Hg^0 from several liters of air using gold amalgamation over the duration of several minutes, followed by thermal dissociation of collected Hg^0 for measurements and analysis by atomic fluorescence or absorption spectroscopy (e.g., Model 2537B, Tekran Inc., Toronto, Canada; typical time resolution of 2.5 to 5 min). Laser-induced fluorescence (LIF) has been developed as a promising alternative technique for the detection of mercury in laboratory studies with detection limit of 0.4 ng m^{-3} for a 1 s integration (Bauer et al., 2003).

Our current understanding of mercury dynamics in the atmosphere and surface exchange processes is hindered by the low time resolution of mercury sensors leading to substantial uncertainties in global atmospheric mercury cycling. High-frequency concentrations fluctuations of Hg^0 are likely occurring at sampling intervals (Δ) shorter than the current 2.5-min resolution and may portray important information about atmospheric sources, sinks, and chemical transformation processes. An example of 5-min time resolution measurements of Hg^0 at a DRI's high elevation research facility (Storm Peak Laboratory, 3200 m a.s.l) in the US Rocky Mountains is reported on Fig. 1a and shows Hg^0 concentration enhancement attributed to long-range transport of pollutants from Asian sources (Obrist, et al., 2008). We used Fourier spectral techniques to obtain the power spectral density of this data series in frequency space. The resulting power spectrum is shown in Fig. 1b as a function of frequency, which ranges from 0 Hz to the Nyquist frequency $1/(2\Delta)=1/(10\,\text{min})=1.67\times10^{-3}$ Hz, which is the highest frequency at which information can be obtained. Figure 1b shows that there is no significant drop off of the power spectral density toward the Nyquist frequency, and we expect (but are not able to quantify) significant contributions above the Nyquist frequency. In other words, temporal changes of Hg^0 concentrations faster than the current 5-min time resolution are likely to occur at a significant level, and may contain important information about Hg^0 fluctuations which are not measureable with current sensors. We expect that a fast-response sensor will hence lead to major progress in air mass characterization

such as in the study mentioned above (Obrist et al., 2008). Other potential applications include quantification of Hg^0 emission and deposition fluxes with micrometeorological techniques (e.g., Eddy Covariance) that require high measurement frequencies (e.g., 1 to 10 Hz), characterization of in situ and laboratory chemical and physical transformation pathways of mercury (i.e., tropospheric oxidation of Hg^0), and characterization of global transport patterns and atmospheric mercury residence notably by spatially resolved airborne measurements.

Gaseous elemental mercury is a unique atmospheric pollutant that occurs in the form of individual mercury atoms in contrast to virtually all other atmospheric pollutants that occur in molecular form. As a consequence, the transition strength of Hg^0 absorption lines is concentrated in individual, narrow lines not split into a multitude of vibrational-rotational lines, and therefore Hg^0 absorption lines are much stronger than the usual molecular absorption lines. Therefore, absorption measurements are a promising approach to measure mercury concentrations and cavity ring-down spectroscopy (CRDS), a sensitive absorption measurement method, which employs very long absorption path lengths in compact cavities (e.g., Berden et al., 2000), is especially well suited to detect atmospheric Hg^0 concentrations and fluxes. CRDS has been investigated previously for detection of Hg^0 concentrations, although detection limits were too high for most ambient air applications. In this paper we report advances in the development of a new laboratory prototype CRD spectrometer demonstrating a sensitivity of 0.10 ng m^{-3} at a time resolution of 10 s which makes this technique an interesting alternative for use in ambient air, background concentration studies. We report detailed comparison of CRDS Hg^0 absorption measurements with data from the existing Tekran 2537B analyzer and discuss the utility of our CRDS Hg^0 instrument for use in laboratory and field studies.

ACPD
9, 22143–22175, 2009

2 Theory absorption spectroscopy and cavity ring-down detection

2.1 Theory of mercury absorption spectroscopy

Of particular interest for the sensitive detection of Hg^0 with absorption spectroscopy is the $6s^1S_0 \rightarrow 6p^3P_1$ electronic transition from the 6s ground state, to the 6p excited state. An absorption cross section of $3.3\times10^{-14}\,cm^2\,atom^{-1}$ has been reported for this Hg^0 absorption line at 253.65 nm in the ultraviolet (UV) (Spuler et al., 2000, and ref. therein). This line has an approximate full width at half-maximum (FWHM) of 0.005 nm at atmospheric pressure, due to hyperfine splitting and atmospheric pressure broadening resulting in a single peak containing all hyperfine components. The high-resolution structure of the Hg^0 absorption spectrum is dominated by hyperfine splitting due to interactions of the nuclear multipole moments of the seven (five with even and two with odd nuclei numbers) naturally occurring isotopes with their electrons.

Direct absorption spectroscopy of atoms and molecules in the gas phase is powerful tool that can yield absolute concentration measurements. According to Beer's law, the transmittance of light through a path length L (m) of an absorbing medium is given by:

$$T(\nu) = P/P_0 = \exp(-\alpha(\nu) \times L) \quad (1)$$

where P_0 is the optical power before the absorber (W), P is the optical power after the absorber (W), and $\alpha(\nu)$ is the absorption coefficient (m^{-1}) at the frequency ν. The absorption is then given by:

$$A(\nu) = 1 - T(\nu) \quad (2)$$

The absorption lineshape $A(\nu)$ of Hg^0 for a given temperature and pressure can be modeled with a Voigt profile, which is a convolution of Gaussian and Lorentzian components. Detailed theoretical descriptions are available elsewhere (e.g., Finkelstein, 1998; Anderson et al., 2007). Briefly, the Gaussian, or inhomogeneous component, is due to Doppler broadening with a line width proportional to the square root of the

ACPD
9, 22143–22175, 2009

ratio of temperature and atomic weight of mercury. The Lorentzian profile is the homogenous component due to natural lifetime and pressure broadening. The Lorentzian width is the sum of the width of natural lifetime broadening and of collisional broadening (a function of pressure) widths, which have been experimentally determined.

2.2 Cavity ring-down spectroscopy

Conventional absorption spectroscopy is based on the measurement of the change in the optical power during transmission through an absorbing medium according to Beer's law (Eq. 1). Its sensitivity is limited by the temporal noise of the light source or incident optical power because a small change in power due to absorption needs to be quantified. The sensitivity can be improved by measuring optical power relative to the incident power and by using a long absorption path, thereby increasing the absorption signal. Cavity ring-down spectroscopy is a simple, fast, and sensitive absorption technique that measures the relative optical power and implements very long absorption paths in compact CRDS absorption cells. The sample is placed inside a high-finesse optical cavity consisting of highly reflective mirrors. A small fraction of a short laser pulse is coupled into the cavity through one of its mirror, the laser pulse is reflected back and forth inside the cavity with a small fraction of the pulse leaking out of the cavity at every reflection due to residual mirror transmission. If the laser pulse is shorter than the cavity's roundtrip length, no interference occurs.

Optical energy stored in the cavity decays exponentially with time due to extinction between the mirrors and reflection losses at the mirrors (O'Keefe and Deacon, 1988; Ramponi et al., 1988). The power of the light leaking out of the cavity through the one of the mirrors is proportional to the optical energy in the cavity and the decay time of the cavity is determined by measuring the optical power leaking out of the cavity as function of time with a fast detector and fitting an exponential function to it. Note that this technique is in principle not affected by laser noise, defined as pulse-to-pulse fluctuations of the laser power.

CRDS obtains the total cavity extinction, which is the sum of mirror reflection losses,

ACPD
9, 22143–22175, 2009

sample scattering, and sample absorption. Assuming that extinction due to mirror losses and sample scattering are constant, they can be subtracted from the total extinction coefficient, resulting in a calibrated measurement of the absorption coefficient of the sample; the more the sample absorbs, the shorter is the measured decay time. The effective absorption path length depends on the reflectivity of the cavity mirrors and can be very long (up to several kilometers), while the sample volume can be kept rather small (Moosmüller et al., 2005).

2.3 Cavity ring-down signal analysis

For highly reflecting mirrors, the time-dependent CRDS signal $S(t)$ can be written as

$$S(t) = S_0 \exp[-\alpha c t] = S_0 \exp[-(\alpha_{Hg} + \alpha_{BG} + \alpha_M) \times c t] \quad (3)$$

where S_0 is the initial signal (i.e., at t=0) and c is the speed of light. The total extinction coefficient α is the sum of a strongly wavelength dependent Hg^0 absorption coefficient α_{Hg} and two additional terms: a background extinction term α_{BG} due to other gaseous and particulate absorption and scattering and a mirror extinction term α_M. Both of these additional terms are largely wavelength independent within the small wavelength range (i.e., ≈0.01 nm) of interest. The mass concentrations C_{Hg} of Hg^0 can be estimated from a measurement of the absorption coefficient α_{Hg} as:

$$C_{Hg} = \frac{\alpha_{Hg} M_{Hg}}{N_A \sigma_{Hg}} \quad (4)$$

where M_{Hg} is the atomic mass of mercury (200.59 g mol^{-1}), N_A is Avogadro's number and σ_{Hg} is the absorption cross section of Hg^0. The mirror extinction term α_M is a function of the distance L between the two mirrors and mirror reflectivity R with:

$$\alpha_M = \frac{1 - R}{L} \quad (5)$$

ACPD
9, 22143–22175, 2009

The effective path length L_{eff} of this CRD arrangement is given by:

$$L_{\text{eff}} = \frac{1}{\alpha_{\text{Hg}} + (\alpha_{\text{BG}} + \alpha_M)} = \frac{L}{\alpha_{\text{Hg}} L + \alpha_{\text{BG}} L + (1 - R)} \quad (6)$$

where for low Hg^0 concentrations, α_{Hg} can be neglected and if particle and gaseous absorption and scattering losses are small, the effective path length L_{eff} can be estimated as:

$$L_{\text{eff}} = \frac{L}{1 - R} \quad (7)$$

For example, for a mirror reflectivity R of 99.9% and a mirror distance L of 1 m, an effective path length of up to 1 km can be achieved with path lengths increasing and detection becoming more sensitive for mirrors with higher reflectivity.

2.4 Performance of previous cavity ring-down spectrometers for Hg^0 detection

Hg^0 detection with CRDS systems has been demonstrated by previous studies, but the sensitivity and time resolution needed for measurement of ambient Hg^0 concentrations and fluxes in the field have not been achieved. Jongma et al. (1995) pioneered ultraviolet CRDS detection of trace gases including Hg^0 with a frequency-doubled, pulsed dye laser (linewidth of 0.1 cm^{-1}) pumped by a frequency-tripled Nd:YAG laser at 355 nm and a 0.45-m length open path CRDS cavity using mirrors with 99.6% reflectivity. This setup was used to measure Hg^0 background concentrations (i.e., 63 ng m^{-3}) in their laboratory with a noise-equivalent (1σ) detection limit of 9 ng m^{-3} for 3 s averaging time. In addition, nearby absorption lines were identified as the forbidden oxygen (O_2) A←X(7,0) transition (N''=19, Q multiplet). A similar laser system was used later by Tao et al. (2000) and by Spuler et al. (2000). Tao et al. (2000) reported a noise-equivalent (3σ) detection limit of 24 ng m^{-3} over an unspecified averaging time with a 0.56-m length open-path CRD cavity with a 0.18-m sample length and mirrors of 99.7% reflectivity. Spuler et al. (2000) achieved a noise-equivalent (3σ) detection limit of 4.5 ng m^{-3}

over 75 s averaging time with a 1.25 m length closed-path CRDS cavity and mirrors of 99.85% reflectivity and demonstrated interference-free (i.e., from ozone and sulfur dioxide) measurement of Hg^0 at ambient conditions. More recently, Carter (2004) developed a CRDS system for measurement of Hg^0 concentrations in flue gases based on an all solid state, frequency-tripled Alexandrite laser, seeded with a single-mode, external-cavity diode laser, thereby reducing the UV output linewidth from 5 cm^{-1} to less than 0.006 cm^{-1}. Using a 0.65-m length closed-path CRDS cavity and mirrors of 99.7% reflectivity, a sensitivity of 90 ng m^{-3} was achieved over an averaging time of 10 s. Development of alternative plasma sources for CRDS measurement of Hg^0 was reported by Duan et al. (2005) using a dye laser system similar to that of Jongma et al. (1995) and an open-path CRDS cavity with mirrors of 99.72% reflectivity. Their detection limit was 400 ng m^{-3} for an average time of 5 s. Finally, Wang et al. (2005) used a similar system with a 0.78 m length open-path CRDS cavity with mirrors of 99.67% reflectivity and a plasma source filling a 6 mm length of the CRDS cavity with Hg^0. They obtained a noise-equivalent (3σ) detection limit of 2 $\mu g\, m^{-3}$ over an averaging time of 2–5 s. Table 1 summarizes detection limits extrapolated to 1 Hz of previous cavity ring-down spectrometers.

3 Instrument description and laboratory testing

3.1 Laser and optics

A schematic diagram of our CRDS instrument is shown in Fig. 2. This instrument uses a frequency-doubled tunable dye laser emitting pulses at a wavelength of 253.65 nm with a linewidth of ~0.9 GHz and a pulse repetition frequency of 50 Hz. The dye laser system (Newport-Spectra-Physics, Mountain View, CA) consists of a Quanta Ray, Q-switched, frequently-tripled Nd:YAG laser operating at a fundamental wavelength of 1064 nm with 50 Hz pulse repetition frequency and generating output pulses at 355 nm after 3rd harmonic frequency conversion. The 355 nm pulses are used to pump a dye

ACPD
9, 22143–22175, 2009

laser (Model Sirah Cobra) to generate laser pulses at 253.65 nm after frequency doubling. Average UV dye laser power is ∼10 mW corresponding to a pulse energy of 200 μJ/pulse. The dye laser wavelength is tunable over a wide range (215–280 nm) using a computer-controlled Littrow grating in the dye resonator.

The laser beam is mode-matched with an appropriate lens into a 1-m length optical cavity consisting of two highly reflecting plano-concave mirrors. The sample is enclosed in the CRDS cavity by a quartz (SiO_2) coated stainless steel tube that shows no contamination or memory-effect for Hg^0 when flushed upstream with a mercury-free air generator (Tekran unit 1100) and monitored downstream with a 2537B Tekran analyzer (see Sect. 3.4 for more details on analyzer 2537B). The plano-concave UV mirrors (MLD Technologies, Mountain View, CA) have a radius of curvature of 1 m and are mounted with adjustable, sealed mirror mounts (Los Gatos Inc., Los Gatos, CA) to form a stable optical cavity. Mirror reflectivity was determined to be 99.895% from CRDS measurements at 253.65 nm (i.e., at the Hg^0 absorption line) for a cavity filled with ultrapure N_2. In this configuration, absorption due to N_2 can be neglected and total cavity losses are due to mirror reflection losses and to N_2 Rayleigh scattering. The N_2 scattering coefficient at 253.65 nm and laboratory temperature and pressure (i.e., 300 K, 843 mbar, respectively) was estimated as 259.4 Mm^{-1} using values reported by Fröhlich and Shaw (1980).

3.2 Data acquisition and signal processing

The optical energy stored in the cavity is monitored by measuring the optical power leaking through the back cavity mirror (Fig. 2) as function of time with a high-speed photo-multiplier tube (PMT) (H6780; Hamamatsu, Japan). Signals are recorded using a 4 MS s^{-1} data acquisition card (CompuScope 12100, GaGe, Lockport, Illinois, USA) and processed in real time using Labview, a graphical programming environment for instrument control and data acquisition.

ACPD
9, 22143–22175, 2009

3.3 Laser wavelength control using an external mercury cell

Repeatable measurements of Hg^0 concentration using CRDS require precise control and corrections of potential drifts of the UV dye laser wavelength. Setting the laser wavelength to the peak of the Hg^0 253.65 nm absorption line, where most sensitive detection is feasible, was achieved by direct measurement of the absorption signal of Hg^0 in a low-pressure Hg^0 vapor cell. As shown in Fig. 2, a fused silicate plate (ESCO Corp., Oak Ridge, NJ, USA) located before the CRDS cavity allowed for extraction of a small fraction of the laser power, which was further split into two equal power laser beams using a UV beam splitter (Edmund Optics Inc., Barrington, NJ, USA) and signals were measured using two photodiodes (PD1 and PD2, DET10M, Thorlabs, Newton, NJ, USA). One of the laser beams was routed through a low-pressure Hg^0 cell and its power was measured by PD1 with this PD1 signal normalized by the PD2 signal, a measure of laser power to correct for fluctuations of the UV laser power (Fig. 2). The Hg^0 cell consists of a 50 mm long, 8 mm diameter, fused silica tube with two fused silica windows attached at 15° relative to normal to avoid direct back reflections and to reduce etalons effects. Liquid mercury was held in a sealed tube extending from the bottom of the cell, and cell Hg^0 concentration was controlled through temperature control of the liquid mercury using an ice bath at 273 K, prepared following ASTM standard procedure E563–08 (2008). However, the sealed tube was likely to small to allow for cooling of the liquid mercury down to 273 K, as discussed in Sect. 4.1. The photodiode signals were extracted from background noise through time-windowing using two independent Boxcar amplifiers (Daly et al., 1985; Stanford Research Systems, 2001) before data acquisition with a DAQ system (National Instruments, Austin, TX, USA). Control of laser drifts was implemented using the hyperfine structure of the mercury absorption line resolved when using a low pressure Hg^0 cell (i.e., 1.3×10^{-5} Pa). Specifically, the real-time monitoring of the laser power incident on photodiodes PD1 and PD2 allowed for (i) manual locking of the laser wavelength to the peak of the absorption line of the ^{202}Hg isotope before each measurement with an estimated precision of 0.0002 nm, and

(ii) control of potential drifts of the of the UV wavelength during CRDS measurements. However, data collection periods in this study were limited to 10 s time periods (see Sect. 4.2) and laser drift were never observed during these short time scales.

3.4 Gaseous elemental mercury source permeation and comparison to Tekran model 2537B mercury analyzer

To evaluate the performance of the CRDS Hg^0 absorption measurements, a Hg^0 vapor generation system was built to supply a wide range of Hg^0 concentrations to the CRDS instrument and a Tekran Instruments Corp. (Knoxville, TN, USA) Model 2537B analyzer was used for instrument comparison. Controlled trace concentrations of Hg^0 were obtained using a HE-SR 1.7CM permeation tube (VICI Metronics, Inc., Poulsbo, WA, USA) with a certified rate of 31.24±2 ng min^{-1} at 50°C. The permeation tube was kept at constant temperature (50°C) using a temperature regulated water bath (Cole Parmer, Vernon Hills, IL, USA), and the permeation flow was controlled to adjust the flushing rate above the tube resulting adjustable source concentrations of Hg^0. A small fraction of this primary Hg^0 source was diluted with mercury-free air (Air-Zero filter; model Tekran 30-25150-00) with flows regulated by two mass flow meter (Aalborg, Orangeburg, NY, USA), one dedicated to the concentrated primary Hg^0 source adjustable from 1–10 ml min^{-1} and one dedicated to the Hg^0-free air adjustable from 1.1–10 l min^{-1}. This setup allowed for generation of stable Hg^0 concentrations over a range from well below 1 to 600 ng m^{-3}.

Mass concentrations of Hg^0 vapor generated by this setup were routed in series through the CRDS cell followed by a Tekran 2537B vapor-phase mercury analyzer. The 2537B instrument collects the air stream on two gold cartridges, followed by thermal desorption and detection by cold vapor atomic fluorescence spectrometry at 253.65 nm. Use of dual gold cartridges allowed alternate sampling and desorption, resulting in continuous measurement of Hg^0 on a predefined time base. The model 2537B was recalibrated every 24-h using its internal permeation source and its sample flow rate was set to 1 l min^{-1}. Blanks for the 2537B were measured during each cal-

ibration and these measurements consistently yielded a mercury mass concentration of 0.00 ng m^{-3}. Set-up, accuracy, and precision of this instrument have been evaluated previously (e.g., Schroeder et al., 1995; Ebinghaus et al., 1999) and the manufacturer reports a detection limit for 5 min samples of 0.10 ng m^{-3}.

4 Measured spectral profiles, instrument performance, and instrument comparisons

4.1 Hg^0 spectral profiles and comparisons to theoretical values

CRDS measurements of pressure-broadened absorption spectra between 253.61 nm and 253.66 nm for different Hg^0 concentrations (i.e., 46 to 535 ng m^{-3}) supplied to the CRDS cell are shown in Fig. 3. The Hg^0 absorption line can clearly be located at 253.65 nm and the presence of a series of forbidden oxygen absorption lines is observed between 253.57 and 253.62 nm. Such forbidden oxygen absorption lines in the UV have been reported before by (e.g., Tao et al., 2000). Due to the relatively constant atmospheric O_2 content, such oxygen absorption lines have been used for additional instrument calibration and quality assurance in ambient air as demonstrated for the measurement of aerosol light absorption by Tian et al. (2009). The insert panel of Fig. 3 shows details of absorption measurements at 253.65 (i.e., at the Hg^0 absorption line) for Hg^0 concentrations of 0 ng m^{-3} (flushed with mercury-free air) and 46 ng m^{-3}. These measurements clearly observe a residual absorption peak at a wavelength of only +0.001 nm above the mercury absorption peak. This peak is very likely due to oxygen absorption as it disappears for a N_2-filled cell.

Figure 4 shows direct (i.e., non-CRDS) transmission spectra from 253.64 to 253.66 nm for mercury cells either filled with high (i.e., 80 kPa; near ambient) N_2 pressure or evacuated to low (i.e., 1.3×10^{-5} Pa) pressure. Specifically, Fig. 4 reports ratios between PD1 and PD2 voltages rescaled to remove reflection losses on the two uncoated windows surfaces of each cells (20% losses estimated from signal without cells

ACPD
9, 22143–22175, 2009

present) and normalized. The 80 kPa profile is clearly pressure broadened, while the low-pressure profile reveals the hyperfine structure of the $^1S_0$-$^3P_1$ transition of Hg^0 with the presence of five distinct absorption isotope peaks as described by others (Spuler et al., 2000; Carruthers et al., 2005; Anderson, et al., 2007; Scheid et al., 2007).

Theoretical absorption coefficients as a function of wavelength for Hg^0 were calculated using a computer program based on previous work by Finkelstein (1998). This model includes Lorentzian and Gaussian linewidth components described above in Sect. 2.1. Specifically, a mercury self-pressure broadening coefficient of 7.60×10^4 Hz Pa^{-1} (Finkelstein, 1998) and a foreign-pressure broadening coefficient of 7.46×10^4 Hz Pa^{-1} for atomic mercury broadened by N_2 (Anderson et al., 2007) were used. We validated our model and its parameterization by modeling a published spectrum (Scheid et al., 2007), which was obtained with a very narrowband (e.g., laser linewidth of about 10 MHz), continuous-wave, solid-state laser. Because we used a spectrally much wider pulsed dye laser, we additionally accounted for laser linewidth and shape in the calculations to reproduce our absorption spectra. A large number of model spectra using different combination of laser linewidth, shape, and cell temperature were generated and the best fit was determined by minimizing the sum of the squared differences between measurements and model value for 0.1 GHz frequency resolution spectra. Specifically, Gaussian and Lorentzian contributions to the laser linewidth from 0 to 3 GHz were included and temperature was varied between 273 and 290 K. The mercury vapor pressure in a Hg^0 cell depends on the temperature of liquid mercury held in a sealed tube extending from the bottom of the cell and maintained in an ice bath. It is likely that the sealed tube used by us was too small for efficient cooling of the liquid mercury down to 273 K, as previously observed by Anderson et al. (2007) with a similar setup. The best fit of our high pressure measured spectra is shown on Fig. 4 and was obtained for 280 K and a laser linewidth modeled with Gaussian and Lorentzian contributions with full-widths-at-half-maximum (FWHM) of 1.8 and 0.2 GHz, respectively. Figure 4 shows that our modeled and experimental spectrums for the high pressure (i.e., 80 kPa) Hg^0 cell are in excellent agreement. As expected, our

ACPD
9, 22143–22175, 2009

modeled laser FWHM was about twice the factory specification of 0.9 GHz reported for the Sirah Dye laser operating in the green, before frequency doubling. Finally, modeling our absorption measurements led to an absorption cross section for Hg^0 of 2.4×10^{-14} cm^2 $atom^{-1}$, a value lower than the value of 3.3×10^{-14} cm^2 $atom^{-1}$ previously reported by Spuler et al. (2000).

The experimental absorption spectrum for the low pressure (i.e., 1.3×10^5 Pa) Hg^0 cell, also reported in Fig. 4, clearly shows the hyperfine structure of the Hg^0 absorption with its five individual peaks. However, peak absorption at low Hg^0 pressure is less than at high pressure, likely due to saturation of the transition at our relatively high laser power due to slower relaxation to the ground state than at high pressure because of the greatly reduced collision frequency. As saturation of the transition is currently not included in our spectral model, the low pressure spectra were not modeled.

The distinct peak of the ^{202}Hg isotope absorption at 253.6531 nm wavelength seen in the low pressure spectrum (see label on Fig. 4) is used to exactly position the laser wavelength for Hg^0 absorption measurements using the computer-controlled Littrow grating of the dye laser. The same low-pressure ^{202}Hg absorption peak was also used for wavelength positioning for the differential "off-line" measurement as described in detail below.

4.2 Hg^0 absorption measurements, comparisons with a Tekran 2537B analyzer

The Hg^0 vapor generation system was connected to the CRDS cavity to supply a range of Hg^0 concentrations and a Tekran 2537B analyzer was connected directly downstream of the cavity for corresponding measurements of Hg^0 concentrations with 5-min time resolution. Hg^0 vapor concentrations were supplied to the cavity at a flow rate of 1 l min^{-1} and allowed to stabilize at a constant level for at least 10 min (i.e., 2 sampling cycle of the 2537B analyzer, $\Delta Hg^0 < 0.1$ ng m^{-3}). For each measurement, the system was calibrated for extinction losses other than Hg^0 absorption CRDS losses by shifting the laser wavelength "off-line" of the Hg^0 absorption spectrum as described below. Specifically, Hg^0 absorption was measured in the cavity with CRDS during 10 s

ACPD
9, 22143–22175, 2009

long measurements by tuning the laser wavelength to the peak of the ^{202}Hg hyperfine absorption line as described in Sect. 3.3. To measure the "off-line" background extinction (i.e., extinction losses other than Hg^0 absorption: mirror losses, α_M, and background extinction, α_{BG}; see Eq. 3), the laser wavelength was shifted by −0.02 nm off the peak ^{202}Hg absorption (i.e., off-line) immediately after the "on-line" measurements using a computer-controlled Littrow grating in the dye laser. Hg^0 absorption was determined as a differential measurement between these on-line and off-line absorption measurements, and measurements were repeated six times for each Hg^0 concentration shown in Fig. 4. In addition, differential measurements of the cell supplied with Hg^0-free air were performed to measure the background extinction difference between "on-line" and "off-line" measurements in the absence of Hg^0, and all data were corrected for this offset.

The vapor generation system allowed supplying Hg^0 concentrations ranging from 0.2 to 573 ng m^{-3}. Our generation vapor setup provided very stable Hg^0 concentrations during periods as long as 30 min, generally within a 0.05 ng m^{-3} range as assessed by 5-min resolution Hg^0 Tekran measurements. Figure 5a–d shows direct comparisons between Hg^0 absorption coefficients α_{Hg} obtained from the CRDS and Hg^0 concentrations as measured by the 2537B analyzer over the range tested. We observed excellent linear correlations between CRDS measurements and the 2537B analyzer over the whole range of Hg^0 concentrations with a coefficient of variability, r^2, of over 0.99 and a linear slope of 6.03 Mm^{-1}/ng m^{-3}. Only Hg^0 concentrations lower than 50 ng m^{-3} (Fig. 5b, 90% of the data) were considered to accurately evaluate the slope and avoid bias due to higher and isolated values. The relationship demonstrated that both analyzers show an excellent, linear response over a large range of Hg^0 concentrations, which is an impressive result given the different mechanism of detection of the two approaches (i.e., pre-concentrations and atomic fluorescence detection versus CRDS detection). Figure 5c details the performance of the CRDS at low-level Hg^0 concentrations in the 0.2 to 6 ng m^{-3} range, with a particularly important range of below 1.7 ng m^{-3} representing sub-ambient Hg^0 concentrations. Even at this low

ACPD
9, 22143–22175, 2009

range, the relationship between measured Hg^0 concentrations and CRDS absorption is still highly linear (r^2>0.99). Error bars reported on CRDS absorption data represent three standard errors calculated for a 10 s time resolution (see Sect. 4.3 and Table 2), and Tekran error bars correspond to three times standard deviation of individual 5-min observations (2% of the background concentrations, i.e., $3\times0.03\,ng\,m^{-3}=0.09\,ng\,m^{-3}$, E. Prestbo, personal communication, 2008, Tekran Inc. Canada).

Figure 5d shows results of 1 s CRDS absorption measurements obtained by difference between the last second of each on-line 10 s measurements and the first second of each off-line 10 s measurements. Errors bars reported on Fig. 5d represent 3 standards errors calculated for a 1 s time resolution (see Sect. 4.3 and Table 2). We observed similar mean concentrations at this high temporal resolution and results are still highly linear to respective Hg^0 concentration measurements observed at 5-min resolution. Both Fig. 5c and d, however, indicate that low-level Hg^0 measurements show higher variability between individual replicates, that is, repeated comparisons of CRDS and Hg^0 Tekran measurements with a constant Hg^0 concentration flushed trough the cell. This indicates that either one or both of the two detection methods approaches its sensitivity or detection limits, or that the supply rate of Hg^0 injected to the instruments may show some low-level concentration fluctuations. The section below discussed possible reasons and uncertainties in CRDS detection.

4.3 Theoretical calculation of CRDS Hg^0 detection limits

The pulse-to-pulse laser signal variability of the CRDS Hg^0 absorption losses at 253.65 nm has been used to estimate the sensitivity and detection limits of our CRDS prototype. The detection limit is defined as the threshold where the Hg^0 absorption information is lost in the signal noise (i.e., detection limit is the same as instrument sensitivity for the CRDS approach). At Hg^0 concentrations lower than $50\,ng\,m^{-3}$, we consistently observed a standard deviation of the CRD signal between 3.7–4.6 Mm^{-1}, with an average value of 4.4 Mm^{-1}. Similar pulse-to-pulse variability was also observed

ACPD
9, 22143–22175, 2009

for all baseline measurements, i.e. when the laser wavelength was tuned "off" the mercury absorption line. For higher Hg^0 concentrations, however, pulse-to-pulse variability increased and reached a maximum at 573 ng m^{-3}, at about 2% of the measured absorption signal. The reasons for this increase in pulse-to-pulse noise at higher Hg^0 levels are currently unclear.

Table 2 reports absorption sensitivities (similar to detection limits) in Mm^{-1}defined as three standard errors for different averaging times and based on the mean standard deviation observed for the CRDS signal over more than 200 measurements (i.e., 4.4 Mm 1). Experimental sensitivities in ng m^{-3} also shown in Table 2 were obtained applying the conversion factor determined from comparison of our CRDS instrument with Tekran 2537B analyzer (i.e., 6.03 Mm^{-1}/ng m^{-3}). Theoretical sensitivities in ng m^{-3}, calculated using the Hg^0 absorption cross section of 2.4×10^{-14} cm^2 $atom^{-1}$ determined by modeling of the hyperfine structure of the $^1S_0$-$^3P_1$ mercury transition (see Sect. 4.1) and Eq. (4), were 21% lower than the experimental values reported in Table 2. At 1 Hz, our CRDS prototype shows an experimental sensitivity of 0.31 ng m^{-3}. Since increases in CRDS averaging time (i.e., decreases in time-resolution of the measurements) led to decreases in CRDS detection limit, this value greatly decreases with longer average times, e.g., to 0.06 ng m^{-3} at 30 s average times. These detection limits are based purely on pulse-to-pulse signal variability and many other factors may make it challenging to reach such low detection limits. The calculation, however, holds promising evidence that the CRDS approach is a feasible technology for use in ambient-level and below-background atmospheric Hg^0 studies.

5 Challenges and uncertainties in measurements

5.1 Uncertainty in Hg^0 absorption cross section

Calculations of Hg^0 concentrations based on CRDS absorption measurements and using Eq. (4) with a Hg^0 absorption cross section, σ_{Hg}, of 2.4×10^{-14} cm^2 $atom^{-1}$, would

yield a conversion factor of 7.33 $Mm^{-1}/ng\,m^{-3}$. Consequently, Tekran-based Hg^0 concentrations (i.e., experimental approach) are 21% higher that Hg^0 concentrations predicted by the theory. Using the higher value of σ_{Hg}, $3.3\times10^{-14}\,cm^2\,atom^{-1}$, reported by Spuler et al. (2000) would further increase the discrepancies between theoretical and experimental based Hg^0 concentrations. Currently, we do not know the reasons for these discrepancies. The accuracy and precision of the Tekran 2537B analyzer has been evaluated in a number of studies (e.g., Schroeder et al., 1995; Ebinghaus et al., 1999). It is hence possible that there may be some inherent problem with the modeling approach used for calculation of the Hg^0 absorption cross section in our study. Further development of our absorption model including saturation processes should allow for modeling of the low pressure spectra, and thus help to evaluate this problem.

5.2 Variability of repeated CRDS absorption measurements at constant Hg^0 levels

Figure 5c shows that at low Hg^0 concentrations between 0.2 and 6 $ng\,m^{-3}$, some variability was observed in multiple 10 s CRDS absorption measurements that were tested within respective 5-min duration Tekran observations. An inherent problem in advancing temporal resolutions of sensors is that high-frequency comparisons to lower time-resolution sensors are impossible. It is hence possible that the variability of repeated CRDS absorption signals at seemingly constant Hg^0 levels could be due to true high temporal resolution fluctuations in Hg^0 concentrations during measurements, and that the Hg^0 supply source – seemingly delivering constant Hg^0 concentrations when time averaged and quantified over the 5 min duration of the Tekran measurements – exhibits fluctuations Hg^0 concentrations. To assess this possibility, we investigated at 253.65 nm (i.e., at the Hg^0 line) the temporal variability of the CRDS absorption signals over a 5-min time span while stable Hg^0 vapor concentrations were supplied to the cavity by the permeation system (0.8 $ng\,m^{-3}$, $\Delta Hg^0 < 0.1\,ng\,m^{-3}$ over four sampling cycles of the 2537B analyzer). Figure 6 shows temporal variability in total absorp-

tion at different sampling frequencies. For each time resolutions reported, we evaluated the maximum difference between the absorption value averaged over 5 min (i.e., 1297.87 Mm^{-1}) and individual absorption values. Fluctuations of individual measurement from the 5-min averaged value were always lower than our instrument detection limits estimated previously for the corresponding time resolutions (cf. Sect. 4.3 and Table 2). For example, maximum variation between the 10 Hz absorption signal and the 5-min average was 0.46 Mm^{-1}, when we estimated our instrument detection limit at 10 Hz to be 0.59 Mm^{-1}.

These results indicate that the Hg^0 supply source was stable, and higher frequency temporal variations in Hg^0 concentrations were unlikely to affect our instrument comparisons. We used a cavity that was sealed air-tight for several hours and was hence removed from potential Hg^0 concentration fluctuations from permeation source and the environment to further investigate the temporal variability in absorption signal over 5-min periods. We observed similar patterns as the ones reported in Fig. 6, confirming that the variability in multiple CRDS absorption measurements may be due to system fluctuations discussed in the following section. Interestingly, direct evaluations of standard deviations of the absorption signals at all time resolutions reported in Fig. 6 agree well with previously reported sensitivities (Table 2) based on the 50 Hz standard deviation (divided by the square root of the number of averaged measurements). These experimental data thus confirm the scaling of our CRDS prototype detection limit with the inverse square root of averaging time.

5.3 Possible interferences due to background/mirror extinction fluctuations, unstable baseline absorption losses, and laser wavelength tuning

During "online-offline" wavelength tuning using the computer-controlled Littrow grating in dye resonator, we noticed slight offsets in absorption baseline losses in spite of careful locking of the laser wavelength to the peak absorption line of the ^{202}Hg isotope in the low pressure Hg^0 cell. We estimate such offset to be low (in the range of ~0.1% of the baseline absorption), but this effect could also contribute to variability when the

ACPD
9, 22143–22175, 2009

CRDS operates close to the detection limit.

Equation (3) shows that the total measured CRDS signal extinction is not only dependent on Hg^0 absorption coefficient (α_{Hg}) but also on (i) background extinction due to other gases and/or particulate absorption and scattering (α_{BG}) and (ii) extinction due to mirror losses (α_M). To calibrate for these losses, we performed differential "on-line/offline" measurements through wavelength tuning with the assumption that these losses (i.e., α_{BG} and α_M) stay constant over the short wavelength shift of 0.02 nm. If losses are dependent even to a low degree on the wavelength shift this may cause some variability, specifically at low Hg^0 concentrations where the Hg^0 absorption coefficient (α_{Hg}) is extremely small as compared to these other extinction losses. Further, if α_{BG} and α_M are not perfectly stable in time, a differential on-line/off-line tuning following a 10 s measurement time may not be fully accurate. We are working on implementation of a fully automated "online/offline" switching procedure on a pulse-to-pulse basis (i.e., at 50 Hz) using a custom piezo controller, allowing for a differential measurement at a time resolution of 25 Hz, which will also continuously adjust for system extinction losses other than Hg^0.

As mentioned in Sect. 4.2, measurements of CRDS absorption losses were adjusted by a baseline value when the cavity was filled with Hg^0-free air and which was determined once per day. Although these adjustments were very small and similar to each other (i.e., $-0.99\pm0.19\,Mm^{-1}$), some differences in Hg^0-free cell absorption values were observed. This variability indicates the presence of possible low-level interferences (e.g., by gaseous constituents, etalon effects, or others) contributing to observed CRDS absorption fluctuations. Finally, other instrument characteristics such as ring-down signal analysis fitting procedures may also contribute to instrument noise and limit current instrument sensitivity. The use of mirrors with a reflectivity higher than that of our current mirrors (i.e., reflectivity of 99.895%) would greatly reduce the influence of most problems discussed above. Such improvements in mirror reflectivity will lead to direct improvement of system detection limits and sensitivity by effectively reducing mirror extinction losses and extending absorption pathlengths according to Eqs. (6)

and (7).

6 Conclusions and future developments

A laboratory CRDS system with greatly improved sensitivity and capabilities for the fast–response, sensitive detection of atmospheric mercury has been demonstrated and discussed. Table 1 summarizes detection limits extrapolated to 1 Hz of our CRDS system, previous CRDS and LIF spectrometers, and analyzers 2537B and RA-915+. Current instrument performance shows similar sensitivity and detection limit to the frequently used Tekran analyzer 2537B, albeit at higher time resolutions. Our CRDS laboratory prototype shows that measured Hg^0 absorption is highly linearly related to Hg^0 concentrations detected by Tekran 2537B analyzer over a Hg^0 concentration range of four orders of magnitude, from 0.2 to 573 $ng\,m^{-3}$. Some variability and uncertainties exist at low concentrations (e.g., <5 $ng\,m^{-3}$), which may be due to instability of our CRDS or laser system, interferences by other gases, unstable Hg^0 permeation concentrations, or others. Another remaining challenge is to better reconcile the theoretical calculations of Hg^0 concentrations using reported and modeled Hg^0 absorption cross sections with concentrations measured using a Tekran 2537 mercury sensor. This issue, however, could be avoided by direct cross-calibration of our CRDS system with a Tekran analyzer 2537B.

With an experimental sensitivity of 0.10 $ng\,m^{-3}$ at a 10 s time resolution, our prototype may evolve in a real time sensor for atmospheric gaseous elemental mercury. Notable improvements to the instrument performance currently under way include (i) automatic pulse-to-pulse tuning for differential "online/offline" wavelength measurements using a custom piezo controller; (ii) optimizing the cavity design with implementation of an open-path cavity for applications such as eddy covariance measurements; (iii) integration of the sensor into a mobile rack and fiber coupling of the laser signal into the cavity for easy field deployment of the system; and (iv) development and use of higher reflectivity mirrors to further advance sensitivity of CRDS measurements.

ACPD
9, 22143–22175, 2009

Acknowledgements. This research has been funded by the NSF EPSCoR program, and the NSF Major Research Instrumentation Program (grant #0923485). We thank R. Parashar for help in C^{++} programming, R. Purcell for help in development of the Hg^0 vapor generation system, M. Scheid for sharing information about his previous measurements of Hg^0 absorption spectrum, G. Tian for his help with Labview software development, and A. Yalin for providing an initial version of the code used for Hg^0 absorption line modeling.

References

Anderson, T. N., Magnuson, J. K., and Lucht, R. P.: Diode-laser-based sensor for ultraviolet absorption measurements of atomic mercury, Appl. Phys. B-Lasers O., 87(2), 341–353, doi:10.1007/s00340-007-2604-z, 2007.

ASTM: Standard practice for preparation and use of an ice-point bath as a reference temperature, E563-082008.

Bauer, D., D'Ottone, L., Campuzano-Jost, P., and Hynes, A. J.: Gas phase elemental mercury: a comparison of LIF detection techniques and study of the kinetics of reaction with the hydroxyl radical, J. Photoch. Photobio. A, 157, 247–256, doi:10.1016/S1010-6030(03)00065-0, 2003.

Berden, G., Peeters, R., and Meijer, G.: Cavity ring-down spectroscopy: experimental schemes and applications, Int. Rev. Phys. Chem., 19(4), 565–607, 2000.

Carruthers, A. E., Lake, T. K., Shah, A., Allen, J. W., Sibbett, W., and Dholakia, K.: Single-scan spectroscopy of mercury at 253.7 nm by sum frequency mixing of violet and red microlensed diode lasers, Opt. Commun., 255(4–6), 261–266, doi:10.1016/j.optcom.2005.06.009, 2005.

Carter, C. C.: A Cavity Ring-Down Spectroscopy Mercury Continuous Emission Monitor, Sensor Research and Development Corporation, Orono, Maine 04473, 118 pp., 2004.

Daly, E. J., Williamson, G. I., Rusbridge, M. G., and Jacobson, A. R.: The boxcar method for the analysis of non-gaussian random signals, Plasma Phys. Contr. F., 27(7), 761–775, 1985.

Duan, Y. X., Wang, C. J., Scherrer, S. T., and Winstead, C. B.: Development of alternative plasma sources for cavity ring-down measurements of mercury, Anal. Chem., 77(15), 4883–4889, doi:10.1021/ac050704x, 2005.

Ebinghaus, R., Jennings, S. G., Schroeder, W. H., Berg, T., Donaghy, T., Guentzel, J., Kenny, C., Kock, H. H., Kvietkus, K., Landing, W., Muhleck, T., Munthe, J., Prestbo, E. M., Schnee-

berger, D., Slemr, F., Sommar, J., Urba, A., Wallschlager, D., and Xiao, Z.: International field intercomparison measurements of atmospheric mercury species at Mace Head, Ireland, Atmos. Environ., 33(18), 3063–3073, 1999.
Finkelstein, N.: An ultraviolet laser source and spectral imaging filters for non-intrusive laser-based diagnositc, PhD thesis, Princeton University (Mechanical and aerospace engineering), 232 pp., 1998.
Frohlich, C. and Shaw, G. E.: New determination of Rayleigh-scattering in the terrestrial atmosphere, Appl. Opt., 19(11), 1773–1775, 1980.
Jongma, R. T., Boogaarts, M. G. H., Holleman, I., and Meijer, G.: Trace gas-detection with cavity ring down spectroscopy, Rev. Sci. Instrum., 66(4), 2821–2828, 1995.
Moosmüller, H., Varma, R., and Arnott, W. P.: Cavity ring-down and cavity-enhanced detection techniques for the measurement of aerosol extinction, Aerosol Sci. Technol., 39, 30–39, doi:10.1080/027868290903880, 2005.
O'Keefe, A. and Deacon, D. A. G.: Cavity ring-down optical spectrometer for absorption-measurements using pulsed laser sources, Rev. Sci. Instrum., 59(12), 2544–2551, 1988.
Obrist, D., Hallar, A. G., McCubbin, I., Stephens, B. B., and Rahn, T.: Atmospheric mercury concentrations at Storm Peak Laboratory in the Rocky Mountains: evidence for long-range transport from Asia, boundary layer contributions, and plant mercury uptake, Atmos. Environ., 42(33), 7579–7589, doi:10.1016/j.atmosenv.2008.06.051, 2008.
Ramponi, A. J., Milanovich, F. P., Kan, T., and Deacon, D.: High-sensitivity atmospheric transmission measurements using a Cavity Ringdown technique, Appl. Optics, 27(22), 4606–4608, 1988.
Scheid, M., Markert, F., Walz, J., Wang, J. Y., Kirchner, M., and Hansch, T. W.: 750 mW continuous-wave solid-state deep ultraviolet laser source at the 253.7 nm transition in mercury, Opt. Lett., 32(8), 955–957, 2007.
Schroeder, W. H., Keeler, G., Kock, H., Roussel, P., Schneeberger, D., and Schaedlich, F.: International field intercomparison of atmospheric mercury measurement methods, Water Air Soil Pollut., 80, 611–620, 1995.
Schroeder, W. H. and Munthe, J.: Atmospheric mercury – an overview, Atmos. Environ., 32(5), 809–822, 1998.
Spuler, S., Linne, M., Sappey, A., and Snyder, S.: Development of a cavity ringdown laser absorption spectrometer for detection of trace levels of mercury, Appl. Optics, 39, 2480–2486, 2000.

Stanford Research Systems: Application Note #4: photon counting, lock-in detection, or Boxcar averaging, Sunnyvale, CA, 2001.

Tao, S. Q., Mazzotti, F. J., Winstead, C. B., and Miller, G. P.: Determination of elemental mercury by cavity ringdown spectrometry, Analyst, 125(6), 1021–1023, 2000.

Tian, G., Moosmüller, H., and Arnott, W. P.: Simultaneous photoacoustic spectroscopy of aerosol and oxygen A-band absorption for the calibration of aerosol light absorption measurements, Aerosol Sci. Technol., 43, 1084–1090, doi:10.1080/02786820903170972, 2009.

Valente, R. J., Shea, C., Humes, K. L., and Tanner, R. L.: Atmospheric mercury in the Great Smoky Mountains compared to regional and global levels, Atmos. Environ., 41(9), 1861–1873, doi:10.1016/j.atmosenv.2006.10.054, 2007.

Wang, C. J., Scherrer, S. T., Duan, Y. X., and Winstead, C. B.: Cavity ringdown measurements of mercury and its hyperfine structures at 254 nm in an atmospheric microwave plasma: spectral interference and analytical performance, J. Anal. Atom. Spectrom., 20(7), 638–644, doi:10.1039/b504318b, 2005.

Table 1. Overview of detection limits extrapolated to 1 Hz for Hg_0, including previous cavity ring-down and laser induced fluorescence spectrometers, analyzers Tekran 2537B and Lumex RA-915+, and our prototype.

Instruments and references		Detection limit ($ng\,m^{-3}\,Hz^{-1/2}$)
Cavity ring-down spectrometry		
	Jongma et al. (1995)	15.6
	Spuler et al. (2000)	39
	Carter et al. (2004)	285
	Duan et al. (2005)	894
	Wang et al. (2005)	3714
	This study	0.31
Laser induced fluorescence spectrometry		
	Bauer et al. (2003)	0.4
Cold vapor atomic fluorescence spectrometry		
	2537B, Tekran	1.7[a]
Atomic absorption spectrometry		
	RA-915+, Lumex	1.6

[a] Extrapolated from a 0.1 $ng\,m^{-3}$ detection limit at a 5-min time resolution.

Table 2. Detection limits – equivalent to sensitivities – of the CRDS prototype at different time resolution. Absorptions (Mm^{-1}) were converted to concentrations ($ng\,m^{-3}$) using the conversion factor measured during comparison with 2537B Tekran gas-phase analyzer (experimental approach).

Time resolution (s)	Sensitivity, detection limit (Mm^{-1})	Experimental sensitivity, detection limit ($ng\,m^{-3}$)
0.1	5.90	0.98
1	1.87	0.31
10	0.59	0.10
30	0.34	0.06

ACPD
9, 22143–22175, 2009

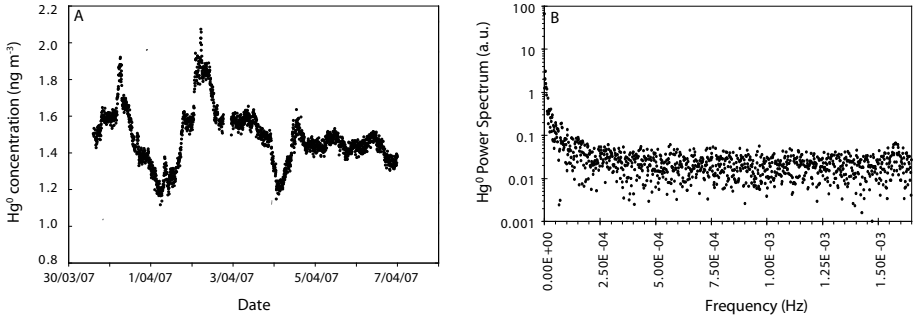

Fig. 1. (**A**) High levels of gaseous elemental mercury measured as function of time at Storm Peak Laboratory (3200 m a.s.l.) in the US Rocky Mountains and attributed to long-range transport of pollutants from Asian sources. (**B**) Corresponding power spectral density as function of frequency for Hg^0 concentrations.

ACPD
9, 22143–22175, 2009

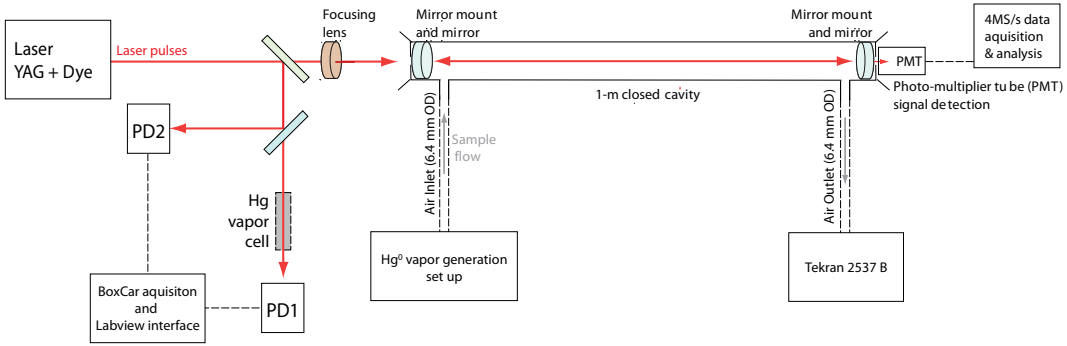

Fig. 2. Schematic overview of CRDS laboratory system.

ACPD
9, 22143–22175, 2009

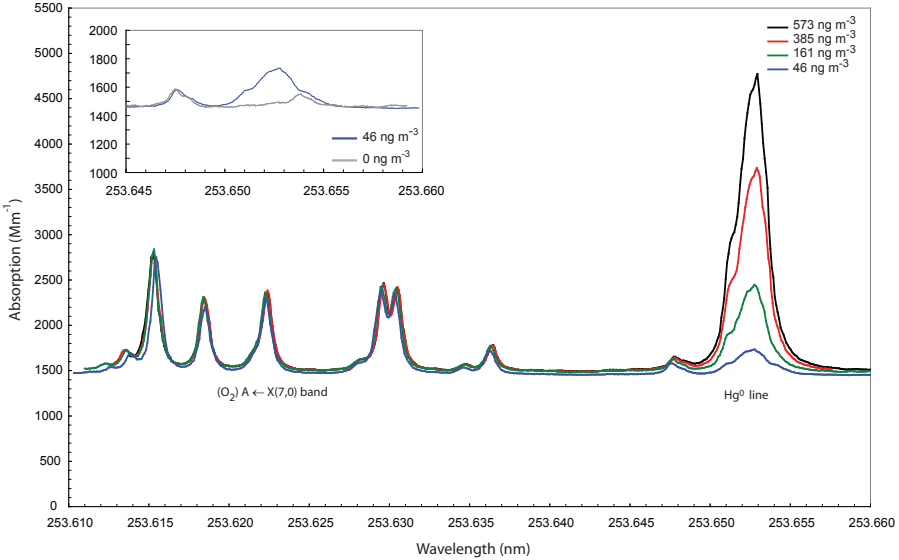

Fig. 3. Wavelength scans of CRDS absorption measured for different Hg^0 concentrations for wavelengths between 253.61 and 253.66 nm. The Hg^0 absorption line is located at 253.653 nm and forbidden molecular oxygen absorption lines are observed between 253.61 and 253.64 nm. A scan of the Hg^0 absorption line measured with a cavity flushed with mercury-free air is reported in insert panel, and shows a residual oxygen absorption line overlapping with the Hg^0 absorption line.

ACPD
9, 22143–22175, 2009

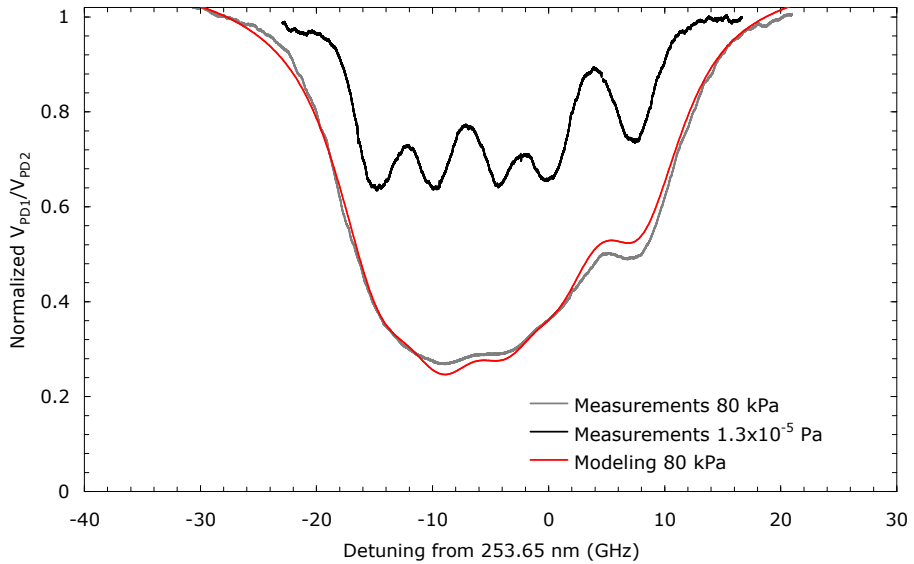

Fig. 4. Absorption spectra of the Hg^0 $^1S_0$-$^3P_1$ transition in a high pressure cell (80 kPa of N_2 buffer gas, grey line) and in an evacuated low pressure cell (1.3×10^{-5} Pa, black line) with a natural isotope mixture. The spectrum from the low pressure cell clearly shows the hyperfine structure of the $^1S_0$-$^3P_1$ transition of Hg^0. A theoretical model of the spectrum from the high pressure cell is shown in red and faithfully reproduces the experimental spectrum.

ACPD
9, 22143–22175, 2009

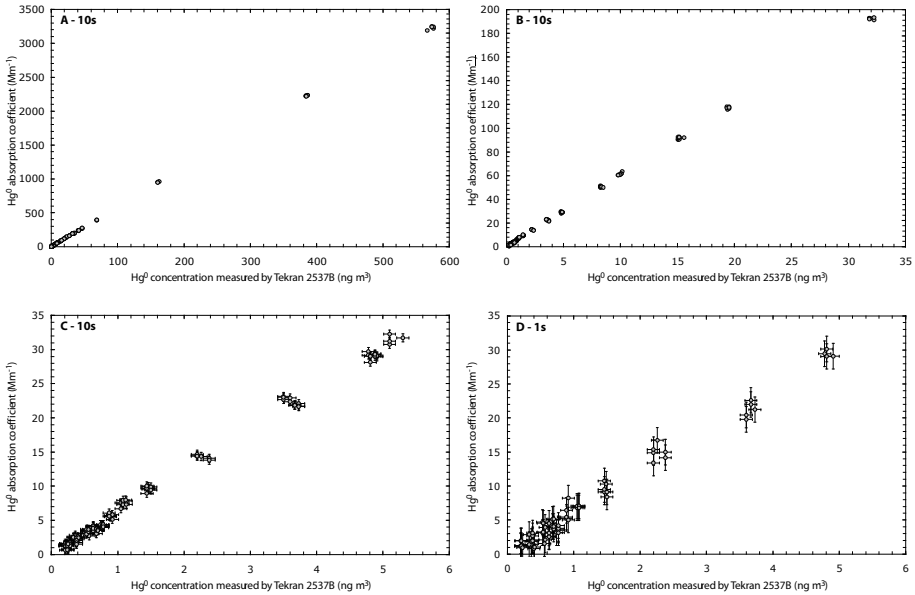

Fig. 5. Direct comparison of Hg^0 absorption coefficients measured by the CRDS system and Tekran 2537B Hg^0 mass concentrations ranging from 0.2 to 573 ng m^{-3} (**A**), from 0.2 to 35 ng m^{-3} (**B**), and from 0.2 to 6 ng m^{-3} (**C**) and (**D**). Panels (A), (B) and (C) report 10 s averaged values, and errors bars are 3 standard errors at a 10 s time resolution. Panel (D) reports 1 s averaged values, and errors bars represent 3 standard errors for a 1 s time resolution. For all panels, the error bars reported for the Tekran data correspond to 3 standard deviation of individual 5-min observations (i.e., 0.09 ng m^{-3}).

ACPD
9, 22143–22175, 2009

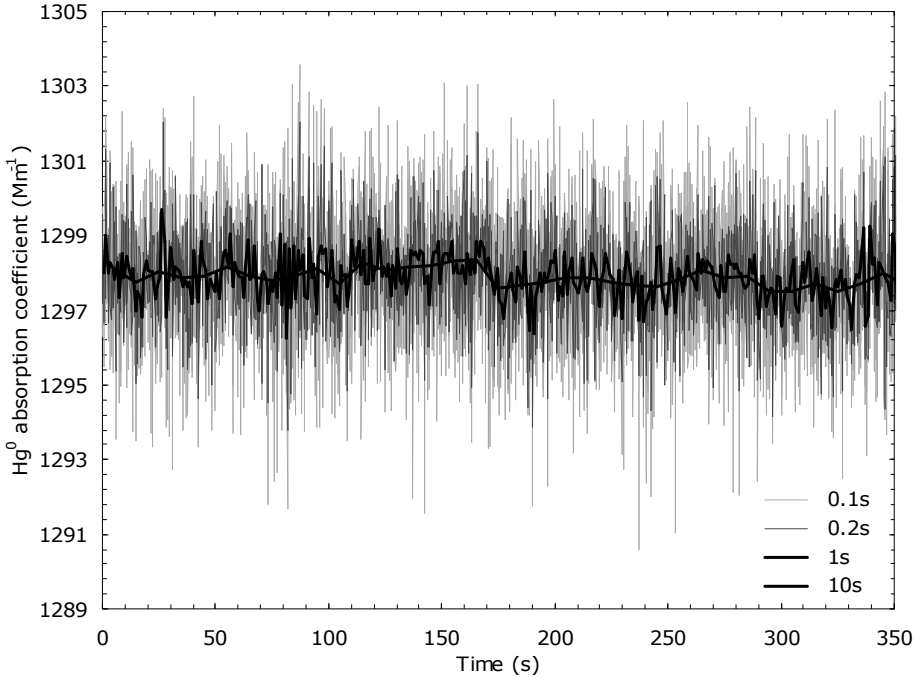

Fig. 6. Temporal variability of the total absorption signal including background and mirror losses at different time resolutions while a stable Hg^0 vapor concentration (i.e., 0.8 ng m^{-3}) was supplied to the cavity over a ~5-min time span.

ACPD
9, 22143–22175, 2009